Quaternary Research 77 (2012) 305–316

Contents lists available at SciVerse ScienceDirect

Quaternary Research

journal homepage: www.elsevier.com/locate/yqres

Single-grain OSL dating of glaciofluvial quartz constrains Reid glaciation in NW Canada to MIS 6

Martina Demuro [a,c,*], Duane G. Froese [b], Lee J. Arnold [a,c], Richard G. Roberts [c]

[a] Centro Nacional de Investigación sobre la Evolución Humana, CENIEH, Paseo de Atapuerca s/n, 09002 Burgos, Spain
[b] Department of Earth and Atmospheric Sciences, University of Alberta, Edmonton, Alberta, Canada T6G 2E3
[c] Centre for Archaeological Science, University of Wollongong, Wollongong, NSW 2522, Australia

ARTICLE INFO

Article history:
Received 3 May 2011
Available online 21 December 2011

Keywords:
Reid glaciation
OSL dating
Single-grain
Glacial deposits
Cordilleran Ice Sheet
Beringia
Ash Bend

ABSTRACT

Improved chronological control on the penultimate advance of the Cordilleran Ice Sheet in northwest Canada (the Reid glaciation) is required for a better understanding of late Quaternary palaeoclimatic and palaeo-environmental change in eastern Beringia. However, reliable dating of glaciation events beyond the last glacial maximum is commonly hindered by a lack of directly dateable material. In this study we (i) provide the first combined minimum and maximum age constraint on the Reid glaciation at Ash Bend, its reference locale in the Stewart River valley, northwestern Canadian Cordillera, using single-grain optically stimulated luminescence dating of quartz; and (ii) compare the timing of the Reid glaciation with other penultimate ice sheet advances in the region with the aim of establishing improved glacial reconstructions in eastern Beringia. We obtain ages of 158 ± 18 ka and 132 ± 18 ka for glaciofluvial sands overlying and underlying the Reid till, respectively. These ages indicate that the Reid advance, at its reference locale, occurred during MIS 6. This precludes an earlier MIS 8 age, and suggests that the Reid advance may have been synchronous with the Delta glaciation of central Alaska, and is likely correlative with the Mirror Creek glaciation in southern Yukon.

Introduction: the 'Penultimate glaciation' problem in eastern Beringia

The extensive non-glaciated portions of the northern Cordillera of Yukon and Alaska, collectively termed eastern Beringia, are fringed by deposits associated with successive advances of the Cordilleran Ice Sheet and local mountain glaciers. The area provides one of the most complete continental glacial records spanning the Late Pliocene through the late Pleistocene, represented by multiple till sheets, glaciofluvial deposits and glaciolacustrine sediments (Hughes et al., 1969; Péwé, 1975; Froese et al., 2000; Kaufman and Manley, 2004; Duk-Rodkin and Barendregt, 2011). For much of this glaciated fringe, the most recent advance associated with marine isotope stage (MIS) 2 (ca. 25–10 ka) (termed the McConnell glaciation in Yukon; Fig. 1) is within the limits of earlier advances (Froese et al., 2000; Kaufman and Manley, 2004; Duk-Rodkin and Barendregt, 2011).

Relatively few of these earlier advances, however, have robust chronologies. This 'penultimate glaciation' problem is common to many areas due to the challenges of establishing reliable age constraints on sedimentary deposits that lie close to, or beyond, the limit of the radiocarbon method (e.g., Pigati et al., 2007). Opportunistic dating strategies have been used at localities that contain suitable deposits for cosmogenic techniques, such as large boulders (e.g., Goehring et al., 2008; Ward et al., 2008; Stroeven et al., 2010), or those that contain overlying, known-age tephras capable of providing minimum age constraints (e.g., Westgate et al., 2001; Ward et al., 2008). However, both these approaches require conditions that are not readily met at many field sites. A case in point is the challenge of defining reliable chronologies for Reid glaciation deposits in Yukon Territory of northwestern Canada.

The multiple, repeated advances of the Cordilleran Ice Sheet that have affected the northern Cordillera of Canada during the Quaternary period were strongly controlled by local topography and consisted of a series of coalescent lobes originating from distinct source areas (Fig. 1). Prominent lobes, including the Selwyn, Cassiar and St. Elias lobes, merged to form a near-continuous carapace of ice during these glacial advances. Although these individual lobes are likely to have had their own ice flow history, the Cordilleran Ice Sheet has been considered as a largely synchronous glacial record with distinct glacial limits assumed to represent consistent advances of the various lobes as a single ice sheet (Hughes et al., 1987; Duk-Rodkin and Barendregt, 2011). In general, the past record of the northern Cordilleran Ice Sheet is one in which the most recent late Pleistocene advances (McConnell glaciation, MIS 2) is fringed by older, more extensive advances. The penultimate glacial limit, the Reid glaciation, is represented by a more extensive moraine and drift complex in

* Corresponding author at: Centro Nacional de Investigación sobre la Evolución Humana, CENIEH, Paseo de Atapuerca s/n, 09002 Burgos, Spain. Fax: +34 947 04 50 66.
E-mail address: martina.demuro@gmail.com (M. Demuro).

0033-5894/$ – see front matter © 2011 University of Washington. Published by Elsevier Inc. All rights reserved.
doi:10.1016/j.yqres.2011.11.009

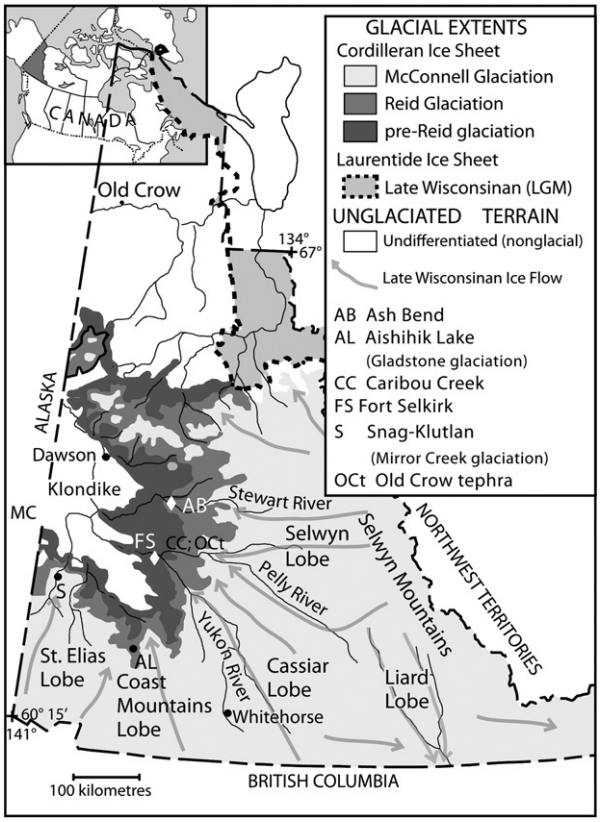

Figure 1. Extent of the McConnell, Reid and pre-Reid glaciations of the Cordilleran Ice Sheet in the Yukon Territory. Also shown are the locations of the Ash Bend site (inset) and the other sites mentioned in the text.

Stewart River valley and has been correlated to other penultimate limits in central and southwestern Yukon (Duk-Rodkin, 1999; Lacelle et al., 2007; Duk-Rodkin and Barendregt, 2011) and Alaska (Begét and Keskinen, 2003). However, at some locations it has been shown that this penultimate glacial limit is likely MIS 4 in age (Ward et al., 2007). Glacial advances that were more extensive than the Reid limits have been termed pre-Reid glaciations, and represent multiple glacial advances of the Cordilleran Ice Sheet as well as local alpine glaciations from the Late Pliocene through the early–middle Pleistocene (Froese et al., 2000; Duk-Rodkin et al., 2010). In this paper we focus on defining a chronology for the Reid glaciation in central Yukon in order to better understand the late Quaternary regional glacial record, particularly the diachronous versus synchronous nature of penultimate glacial advances across eastern Beringia.

A maximum age for the Reid glaciation of 311 ± 32 ka is provided by $^{40}Ar/^{39}Ar$ dating of basalt underlying outwash at Fort Selkirk (Fig. 1), near the confluence of Black Creek and the Yukon River, central Yukon Territory (Huscroft et al., 2004). Minimum age constraints for the Reid glaciation in Yukon Territory are more ambiguous and suggest that Reid deposits likely represent a regionally diachronous record (Ward et al., 2007, 2008). Cosmogenic dating on four boulders from deposits that have been mapped as Reid drift in the Aishihik Lake area, southwest Yukon Territory (Fig. 1), yielded ages of 54 to 51 ka (Ward et al., 2007). That study provided the first chronological evidence for a MIS 4 glacial expansion of the Cordilleran Ice Sheet. This particular glacial expansion, which represents an advance of the St. Elias and Cassiar lobes in southwest Yukon Territory, was subsequently renamed the Gladstone glaciation at the Aishihik Lake locale (Ward et al., 2007). In contrast, Reid deposits found along the Pelly and Stewart rivers, including the Ash Bend site (Fig. 1), in central Yukon Territory, belong to an expansion of the Selwyn Mountain lobe. Evidence for a MIS 6 minimum age for Reid deposits of the Selwyn lobe have been provided along the Pelly River (Caribou Creek; Fig. 1), where silts containing the Old Crow tephra (originally dated to 140 ± 10 ka) are present overlying deglacial Reid gravels (Ward et al., 2008), and from Ash Bend where the ~80 ka Sheep Creek–Klondike tephra (SCt-K) is found overlying Reid till (Westgate et al., 2008). The chronology of the Old Crow tephra has been recently revised to 124 ± 10 ka by Preece et al. (2011) from a new fission track age and improved fission-track dosimetry standard, but it still indicates a late MIS 6 age for the eruption (Reyes et al., 2010). An additional line of evidence suggesting a MIS 6 minimum age for the Reid advance in central Yukon comes from the presence of a distinctive MIS 5e surface soil, the Diversion Creek palaeosol (Smith et al., 1986; Westgate et al., 2001), which commonly overlies glacial outwash deposits in the Stewart River valley. Elsewhere, cosmogenic ages presented by Stroeven et al. (2010) within the Reid limit, but beyond the MIS 2 moraine, indicate a MIS 5 or MIS 6 minimum age for Reid deposits associated with the Selwyn lobe. Taken together, the findings indicate that the Reid drift, which has been frequently mapped as a regionally coherent advance of the Cordilleran Ice Sheet (Duk-Rodkin, 1999), may be a diachronous record in need of detailed re-examination and establishment of improved chronologies (Ward et al., 2007, 2008).

Despite the ambiguities of existing chronologies for the penultimate and earlier advances of the northern Cordillera, broad stratigraphic correlations have been proposed (Duk-Rodkin and Barendregt, 2011) with implications for regional reconstructions of palaeoclimate across northwestern Canada and eastern Alaska. However, the absence of reliable minimum and maximum age constraints directly on such glacial deposits precludes a fuller understanding of their regional climatic significance, and whether they truly represent coherent, synchronous episodes. The aim of this study is, therefore, twofold: (i) to study the OSL characteristics of individual silt-size quartz grains from glacial deposits in this region and to establish reliable chronologies for glacial advances using the latest developments in OSL dating; and (ii) to obtain new and direct chronologies for Reid deposits in central Yukon that can be integrated within the broader, regional glacial record to provide new insights into the spatio-temporal dynamics of the ice sheet advances prior to MIS 2 in eastern Beringia.

Site description

The Ash Bend site, on Stewart River (63°30′N, 137°15′W; 460 m a.s.l.), west-central Yukon Territory (Fig. 1) is located close to the type area for the Reid glaciation (Reid Lakes) as originally defined by Bostock (1966), and is recognised as one of the main reference sections for dating this glacial episode (e.g., Westgate et al., 2001). Ash Bend contains a 10-m-thick recessive sequence of Reid till and glaciofluvial gravels (Figs. 2a–b) overlain by loess deposits containing organic-rich material, bones and tephra layers (Hughes et al., 1987; Westgate et al., 2001, 2008). The till and outwash deposits were described in detail by Hughes et al. (1987), while further work by Westgate et al. (2001, 2008) has refined the lithostratigraphy of the loessal sequence overlying the Reid deposits at a channel cut exposure located towards the downstream end of the section. This overlying loess sequence contains several tephra beds and spans the glacial–interglacial cycle that succeeded the deposition of Reid drift (Schweger, 2003; Westgate et al., 2008).

Two OSL samples were collected from two glaciofluvial beds bracketing the Reid till at Ash Bend (Figs. 2c–d), described herein as Units 1 and 3 (Fig. 2a). Sample 57A was collected from the unit overlying the till (Unit 3), ~6 m below the surface. This unit is a planar–tabular cross-bedded sand deposit formed in a braided river environment. The entire deposit can be characterised as proximal-braided given the low-relief of bar forms (thin planar–tabular cross-beds) observed in the gravel section. Sample 58A was collected about 30 m below the surface from the unit immediately underlying

https://doi.org/10.1016/j.yqres.2011.11.009 Published online by Cambridge University Press

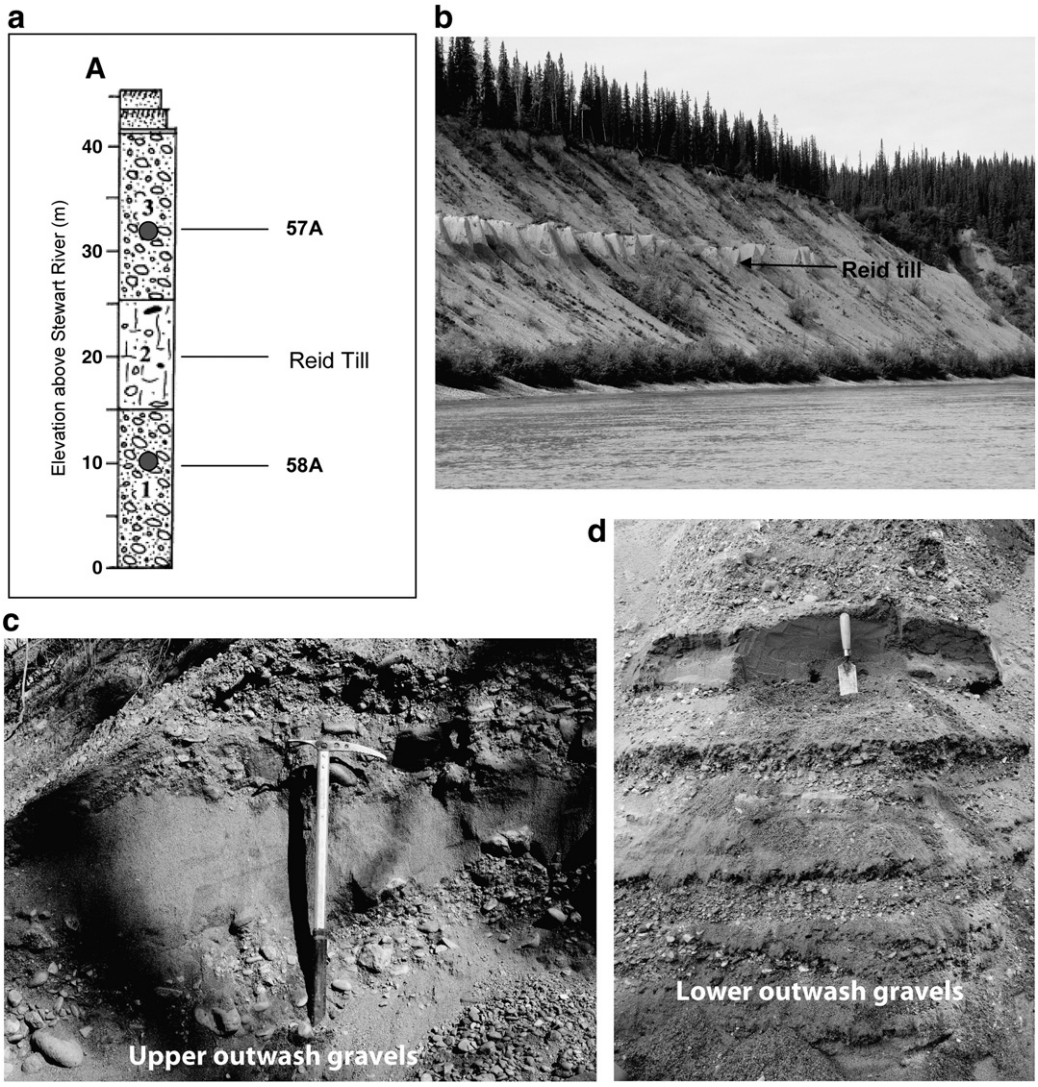

Figure 2. (a) Reid glacial deposits at Ash Bend as described by Hughes et al. (1987) and position of OSL samples from the glaciofluvial gravels (Units 1 and 3) bracketing the Reid till (Unit 2). Examples of (b) Reid till deposits, (c) upper outwash gravels, and (d) lower outwash gravels at Ash Bend site.

the till (Unit 1). The OSL sediment sample was taken from a 25-cm-thick sandy bed within this gravel unit, interpreted as the top sands of a channel bar formed in a braided-river environment.

OSL methodology

The exposed stratigraphy was cut back vertically in order to clean the exposure and to avoid sampling of loose material. Samples were collected by inserting opaque PVC tubes horizontally into the vertically exposed stratigraphy. An additional sediment sample (~200 g) was collected from within a few centimetres of each OSL sample tube for the purposes of dosimetry determination and water-content analysis.

Detailed descriptions of the principles of OSL dating methods can be found elsewhere (Aitken, 1985, 1998; Bøtter-Jensen et al., 2003; Wintle and Murray, 2006) and a general overview of single-grain dating is provided by Duller (2008). Samples were prepared under subdued red light to avoid any depletion of the natural OSL signal. Standard preparation procedures were followed to extract pure coarse-grain (90–125 μm) quartz fractions, as described by Aitken (1998). The quartz extracts were treated with 48% hydrofluoric (HF) acid for 45 min to etch away the outer (~10 μm) alpha-irradiated rinds and to remove any contaminating feldspar grains. The etched quartz fractions were treated with 30% HCl for 45 min to eliminate any acid-soluble fluoride precipitates, and sieved again (using a 63-μm sieve) to remove any disaggregated quartz grains and partially etched feldspars.

OSL measurements were made using a Risø TL-DA-15 reader (Bøtter-Jensen et al., 2003) equipped with an array of blue (470 ± 30 nm) light-emitting diodes (LEDs), delivering > 40 mW/cm^2 at full power, and an infrared (IR, 875 nm) LED array, providing 135 mW/cm^2 at full power. Single-grain OSL signals were stimulated using a green (532 nm) 10 mW Nd:YVO_4 laser delivering ~45 W/cm^2 (90% power) focused on to aluminium discs drilled with a 10 × 10 array of grain holes (300 μm wide and 300 μm deep). Detection of the ultraviolet (UV) emissions was made using a blue-sensitive Electron Tubes Ltd 9235QA photomultiplier tube fitted with a 7-mm-thick Hoya U-340 filter. Samples were irradiated with a $^{90}Sr/^{90}Y$ beta source (average dose rate ~7.5 Gy min^{-1}) calibrated for each grain-hole position across the single-grain disc plane.

Equivalent dose (D_e) estimates were obtained using the single-aliquot regenerative-dose (SAR) protocol described in Murray and Wintle (2000) and modified by Duller (2003) to include a check for contamination of feldspar grains or inclusions (Table 1). The suitability of the SAR measurement conditions presented in Table 1 was tested via dose recovery experiments (Murray and Wintle, 2003) performed on ~800-grain aliquots of sample 57A. The most accurate dose recovery results were obtained using a low temperature regenerative-dose preheat

https://doi.org/10.1016/j.yqres.2011.11.009 Published online by Cambridge University Press

Table 1
Single-aliquot regenerative-dose protocol (SAR) measurement conditions used in this study. A series of regenerative-dose (L_i) and test dose (T_i) OSL measurements are performed on each individual quartz grain to obtain a sensitivity-corrected dose–response curve on to which the sensitivity-corrected natural (L_n/T_n) signal is interpolated to obtain a D_e value. In order to check for contamination of the quartz OSL by feldspar grain or inclusions, a repeat dose point is added, which includes an infrared (IR) bleach performed for 20 s at 50°C prior to the main L_i measurement, as described in Duller (2003).

Step	SAR treatment	Nomenclature
1 [a]	Give dose	L_d
2 [b]	Stimulate with infrared LEDs at 50°C for 20 s at 90% power	
3	Preheat to 160°C for 10 s	
4	Stimulate with green laser at 125°C for 1 s at 90% power	L_i
5	Give test dose	T_d
6	Cutheat of 160°C	
7	Stimulate with green laser at 125°C for 1 s at 90% power	T_i

[a] Step omitted when measuring natural signal.
[b] Step added only when measuring the OSL IR depletion ratio (Duller, 2003).

of 160°C for 10 s and a test-dose cutheat of 160°C, which yielded a mean ratio of recovered to given dose of 0.96 ± 0.06 and a mean recycling ratio of 1.00 ± 0.08 (Figure S1).

For each single-grain D_e estimate, the sensitivity-corrected dose–response curves were constructed using the first 0.08 to 0.3 s of the OSL signal (adjusted for each individual grain according to the shape of the OSL decay curve) minus a mean background count, obtained from the last 0.1 s of stimulation. The integration of the initial OSL signal was varied to avoid the inclusion of the non-decaying part of the signal, and to obtain the most suitable dose–response curve fit to the sensitivity-corrected dose points (i.e., that with the smallest possible curve-fitting error). Sensitivity-corrected dose–response curves were fitted using a saturating-exponential-plus-linear function. Calculation of D_0 (the characteristic saturated dose of the dose–response curve) was carried out by excluding the linear term and fitting a single saturating exponential function to the dose–response curves.

Single-grain D_e estimates were accepted for further analysis if (1) the sensitivity-corrected luminescence response (L_i/T_i) of the 0 Gy regenerative-dose point amounted to less than 5% of the sensitivity-corrected natural signal response (L_n/T_n); (2) the recycling ratios (the ratio of two L_i/T_i values obtained from two equal doses measured initially and at the end of the SAR sequence) were consistent with unity at 1σ; (3) the relative error of the natural test dose signal (T_n) was <30%; (4) The OSL IR depletion ratio (the ratio of the L_i/T_i values obtained from two identical regenerative doses measured with and without prior IR stimulation; Duller (2003)) was consistent with unity at 1σ; and (5) the natural OSL signal intensities (L_n) were >3 standard deviations above the 'late-light' background signal. This final criterion is applied to avoid the inclusion of aberrant '0 Gy' grains that cannot be reasonably explained in terms of the expected depositional context of the samples.

D_e estimates are presented with their 1σ error ranges, which are derived from three sources of uncertainty: (i) a random uncertainty term arising from photon counting statistics of each OSL measurement (L_i and T_i); (ii) an instrumental error term of 2%, which is added in quadrature to each OSL measurement error and describes the random uncertainty associated with instrument reproducibility (Duller, 2007), and (iii) a dose–response curve-fitting error, which is calculated in Analyst v3.24 using 1000 iterations of the Monte Carlo method described by Duller (2007).

Environmental dose rates were determined from the bulk sediments collected immediately adjacent to the main OSL samples using a combination of instrumental neutron activation analysis (INAA) and inductively coupled plasma optical emission spectrometry (ICP-OES). Measured radionuclide concentrations of U, Th and ^{40}K were converted to specific activities and dose rate values (Table 2) using the conversion factors of Adamiec and Aitken (1998) and Stokes et al. (2003).

The present-day water contents for samples 57A and 58A (also expressed as a percentage of dry mass) are 2% and 18%. Both these values are low and are not considered representative of the long-term moisture contents for these samples. The glaciofluvial samples were collected from perennially frozen (permafrost) sections, which typically display present-day moisture contents close to, or in excess of, 30%. Three additional samples (55C, 53C, 52A) collected from the overlying perennially frozen deposits in the same depositional sequence at Ash Bend, for instance, yielded present-day water contents of 40%, 50% and 29%, respectively (though we acknowledge that these samples were taken from finer-grained silt deposits and thus may have been more ice-rich than the Reid glaciofluvial sands). It is possible that some evaporation of moisture took place during exposure and sampling of samples 57A and 58A, which was carried out during the summer months once the freshly exposed, near-surface sediments of the profile had thawed sufficiently. The present-day water-content values for frozen sediments located deeper in the exposure face are likely to be higher, and much closer to field saturation, than the 'as-measured' values obtained for our melted, near-surface samples. Moreover, the higher moisture contents of the former should have prevailed throughout their burial period, as these sediments are thought to have remained permanently in the permafrost zone following initial deposition.

In light of the uncharacteristically low 'as-measured' water contents of samples 57A and 58A, and potential concerns surrounding their representativeness of past burial conditions, we have conservatively used the saturated water content values of these samples to calculate their final dose rates. This approach is consistent with that employed in many other OSL dating studies of coarse-grained, sand-rich, glaciofluvial (or similar) permafrost deposits (e.g., Hansen et al., 1999; Thomas et al., 2006; Houmark-Nielsen, 2008). Uncertainties of 15% and 10% have been assigned to all water and organic content measurements, respectively, to account for potential variations during the burial periods and errors arising from non-identical field and laboratory conditions. The measured saturated water contents for samples 57A and 58A were 30% and 36%, respectively. Table 2 shows the revised environmental dose rates values obtained after adjustments for saturated water contents have been made. The revised dose rate values for these samples have decreased by ~20%, changing from ~1.56 Gy/ka to ~1.25 Gy/ka (see Supplementary material and Table S2).

Results

Single-grain luminescence behaviours

Single-grain OSL measurements were performed on 2300 grains of sample 57A and 2000 grains of sample 58A. Generally, these deposits were dim, with ~70% of quartz grains producing no luminescence (i.e., their T_n OSL signal intensities were <3 standard deviations above background) (Figure S2a). A total of 139 grains in sample 57A and 115 grains in sample 58A produced enough luminescence to construct sensitivity-corrected dose–response curves, which equates to ~6% of the total number of measured grains (Table S1). However, ~83% of these luminescent grains did not pass the SAR rejection criteria, as detailed in Table S1. In total, 23 grains in sample 57A and 20 grains in sample 58A were accepted for final D_e estimation. In general, the T_n signal intensities of the accepted grains were relatively low (<200 counts in the initial 0.3 s of green laser stimulation following a test-dose of 30 Gy) (Figure S2c). The low yield of suitable grains for dating underscores the advantages of using single-grain techniques in this context; this approach ensures that only those few grains considered reliable contribute to the final OSL ages, while the much larger number of grains displaying unsuitable luminescence properties – which would otherwise be included in multi-grain aliquot D_e measurements –

https://doi.org/10.1016/j.yqres.2011.11.009 Published online by Cambridge University Press

Table 2
Radionuclide activities and calculated dose rates for samples 57A and 58A. Dose rates were calculated using the conversion factors of Adamiec and Aitken (1998) and Stokes et al. (2003), and are presented after adjustment for water and organic content.

Sample	Sample depth (m)	Grain size (μm)	Water/ organic content [a,b]	Radionuclide activities [c] (Bq/kg)			Environmental dose rate (Gy/ka)			Total dose rate[e] (Gy/ka)
				^{238}U	^{232}Th	^{40}K	Gamma dose rate	Beta dose rate	Cosmic ray dose rate [d]	
57A	6	90–125	30/1.8	19.4 ± 0.6	15.4 ± 0.5	254 ± 8.0	0.41 ± 0.02	0.66 ± 0.03	0.09 ± 0.01	1.19 ± 0.07
58A	30	90–125	36/1.2	40.0 ± 1.2	21.9 ± 0.7	223 ± 7.0	0.55 ± 0.03	0.74 ± 0.04	0.01 ± 0.001	1.33 ± 0.09

[a] Values represent saturated water contents. Saturated water content was measured in the laboratory using ~100 g of the bulk sediment. Samples were initially dried in a 100°C oven overnight and their dry mass recorded. Enough water was then added to the dry samples to reach interstitial water saturation; that is, ensuring that the inter-grain pore spaces were filled by water without generating excess or freestanding water. The samples were reweighed and the saturated water content was calculated as a percentage of dry sediment mass.

[b] The organic contents (expressed as a percentage of dry mass) were derived through loss of ignition (LOI). For this purpose, ~10 g of dried bulk sediment was weighed before and after being oxidised at 950°C as part of the ICP-OES sample preparation procedure.

[c] Measurements of radionuclide concentrations (ppm for U and Th, and % for K) have been made by INAA/ICP-OES on 10 g of dried and powdered sample and converted to specific activities (Bq/kg) using the conversion factors of Adamiec and Aitken (1998). A relative uncertainty of 3% was assigned to the radionuclide concentrations obtained by ICP-OES and INAA when calculating the beta dose rates. Gamma dose rate uncertainties on U, Th and K were increased to 10% to accommodate any spatial variations in the sedimentary matrix.

[d] Cosmic-ray contributions to the total dose rates were calculated following Prescott and Hutton (1994), taking into account the altitude and geomagnetic latitude of the site, the sample depths, and their water contents.

[e] The final dose rate estimates have been adjusted for beta-dose attenuation (Mejdahl, 1979), sample water content (Aitken, 1985) and organic content (Lian et al., 1995). Dose rate values represent the mean ± total uncertainty (68% confidence interval), calculated as the quadratic sum of the random and systematic uncertainties. The final dose rate estimates include an internal alpha dose rate of 0.03 Gy/ka for each sample, based on measurements made by Bowler et al. (2003), with an assigned relative uncertainty of ±20%.

can be individually identified and excluded from the final age determination.

Examples of sensitivity-corrected dose–response curve and OSL decay curves for two accepted grains from samples 57A and 58A are shown in Figures 3a–b and c–d, respectively. The onset of saturation (D_0) for both dose–response curves is well above the maximum administered dose of ~250 and ~350 Gy, respectively. Analysis of the dose–response curve saturation properties of all 43 accepted grains from these two samples reveals that ~50% have D_0 values >170 Gy, while ~25% of the quartz grains have characteristic saturation dose values of <80 Gy (Fig. 4a). Several accepted quartz grains (n = 6) of samples 57A and 58A also have very high D_0 values of >600 Gy (Figs. 4b–c). The D_0 characteristics of the accepted grains are encouraging because these samples are expected to be ~124 ka or older, and, hence, early onset of dose saturation is not likely to compromise the suitability of OSL dating in this study.

Single-grain D_e distributions and statistical analysis

Two descriptive statistics have been used to quantify the single-grain D_e distribution characteristics (Table 3): (i) overdispersion, which provides a measure of the relative spread in D_e values remaining after taking measurement uncertainties into account (calculated using the central age model of Galbraith et al. (1999)), and (ii) log weighted

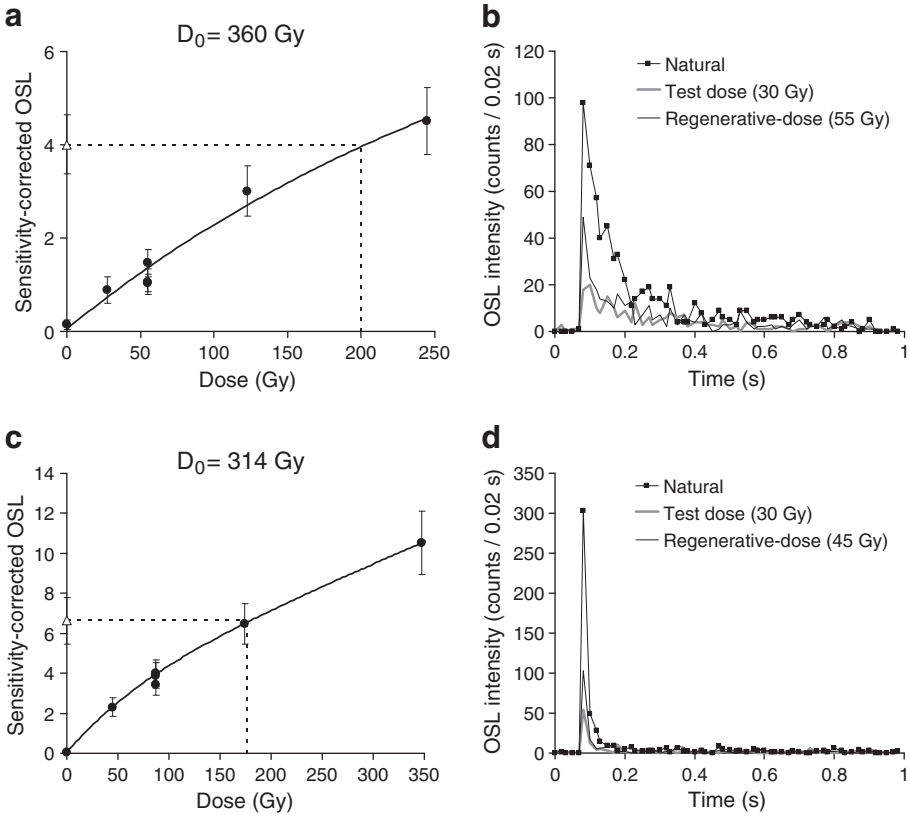

Figure 3. Sensitivity-corrected dose–response curves and corresponding OSL decay curves obtained from individual quartz grains of (a–b) sample 57A and (c–d) sample 58A.

https://doi.org/10.1016/j.yqres.2011.11.009 Published online by Cambridge University Press

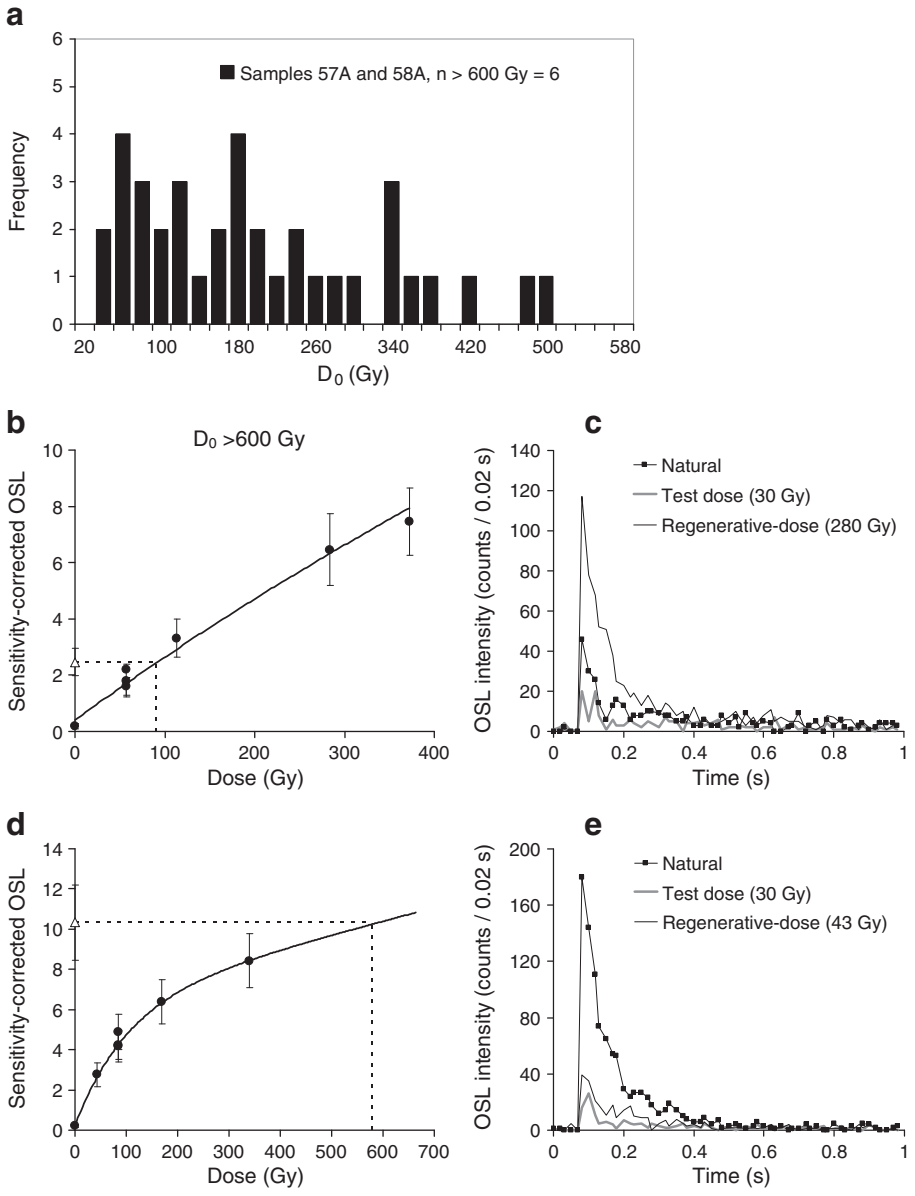

Figure 4. (a) Distribution of D_0 values for accepted single grains of the Reid glaciofluvial gravels, samples 57A and 58A (n = 43). Sensitivity-corrected dose–response curves and corresponding OSL decay curves obtained from individual quartz grains of a grain from sample 57A with D_0 > 600 Gy (b–c), and a high-dose grain of sample 58A (d–e).

Table 3
D_e distribution statistics obtained from single-grain OSL dating of samples 57A and 58A. Also shown are the D_e values and corresponding ages calculated using the central age model (CAM) and the 3- and 4-parameter minimum age models (MAM-3 and MAM-4). D_e values and ages in bold indicate the accepted age model according to the weighted skewness test results.

Sample	Measured/ accepted grains	Overdispersion[a] (%)	Weighted skewness value	Critical skewness[b] 68% C.I.	Critical skewness[b] 95% C.I.	CAM D_e (Gy)	MAM-3 D_e[c] (Gy)	MAM-4 D_e[c] (Gy)	CAM age (ka)	MAM-3 age (ka)	MAM-4 age (ka)
57A	2300/23	35 ± 9	−0.12	0.51	1.02	**187 ± 18**	124 ± 24	139 ± 40	**158 ± 18**	105 ± 22	117 ± 35
58A	2000/20	42 ± 10	0.45	0.55	1.10	**176 ± 21**	98 ± 19	106 ± 38	**132 ± 18**	74 ± 16	79 ± 29

[a] Overdispersion represents the relative spread in D_e values remaining after taking the measurement uncertainties into account, and has been calculated using the central age model of Galbraith et al. (1999).

[b] Weighted skewness was calculated on log-transformed D_e values using Eqs. 7–8 of Arnold and Roberts (2009). Critical skewness scores have been calculated using Eq. 16 of Bailey and Arnold (2006). Single-grain D_e distributions are considered to be significantly positively skewed at 68% C.I. or 95% C.I. if the weighted skewness value is greater than the critical skewness value (Bailey and Arnold, 2006).

[c] Before calculating the MAM-3 and MAM-4 D_e estimates, we added, in quadrature, an overdispersion value of 15% to the individual errors of each single-grain D_e value. This provides an estimate of the inherent dose overdispersion that is typically present in well-bleached sediments that have not been disturbed since burial (e.g., Galbraith et al., 2005; Tables 4–5 in Arnold and Roberts, 2009), and must be taken into consideration to obtain accurate MAM burial dose estimates.

https://doi.org/10.1016/j.yqres.2011.11.009 Published online by Cambridge University Press

skewness, which was used to detect and quantify asymmetric D_e scatter assumed to be associated with heterogeneously bleached sediments (calculated using Eqs. 7 and 8 of Arnold and Roberts (2009), and assessed against the critical skewness values, outlined in Bailey and Arnold (2006)). To obtain representative burial dose estimates from these D_e distributions, we have applied a range of statistical age models — namely, the central age model (CAM) and the three- and four-parameter minimum age models (MAM-3 and MAM-4, respectively) of Galbraith et al. (1999) (Table 3).

Figures 5a–d show the dose distributions for samples 57A and 58A plotted as frequency histograms, with a log-transformed x-axis, and as radial plots centred on the CAM D_e values. The overdispersion values of samples 57A and 58A are $35 \pm 9\%$ and $42 \pm 10\%$, respectively, suggesting that additional sources of extrinsic or intrinsic scatter contribute to the overall spread of these single-grain D_e datasets. However, the dose distributions are not significantly positively skewed at the 68% C.I. or 95% C.I. (Table 3) and do not display a distinct 'leading-edge' of lower D_e values or elongated, asymmetric 'tails' of higher D_e values. As such, these samples do not share the characteristic appearance of partially bleached single-grain D_e distributions commonly reported elsewhere (e.g., Olley et al., 1999, 2004; Arnold et al., 2009).

The CAM D_e values for samples 57A and 58A are 187 ± 18 Gy and 176 ± 21 Gy, respectively, and the corresponding ages obtained using the revised dose rates (calculated with the saturated water contents) are 158 ± 18 ka and 132 ± 18 ka (Table 3; Fig. 6). The CAM ages are stratigraphically reversed but, importantly, are in agreement at $\pm 1\,\sigma$. Both these ages are stratigraphically consistent with the ~80 ka age of the overlying SCt-K found at Ash Bend (Westgate et al., 2008), and are also consistent with the stratigraphic position of the Reid glaciofluvial gravels below the ~124 ka Old Crow tephra at Caribou Creek (Ward et al., 2008). As expected, the MAM ages are younger than the CAM ages for both samples. The MAM-3 and MAM-4 ages for sample 57A are 105 ± 22 ka and 117 ± 35 ka, respectively. The corresponding MAM-3 and MAM-4 ages for sample 58A are 74 ± 16 ka and 79 ± 29 ka (Table 3).The 1σ error ranges of the MAM-3 and MAM-4 age estimates are relatively large (i.e., 20–37%), which reflects the limited number of individual D_e estimates accepted for each sample. The MAM-3 and MAM-4 ages are stratigraphically consistent with the ~80 ka OSL ages obtained by Westgate et al. (2008) on the overlying SCt-K at Ash Bend, however, they are both systematically younger than the ~124 ka age of the overlying Old Crow tephra at Caribou Creek.

Comparison with independent age control suggests that the CAM is the most appropriate age model for analysing these D_e datasets. This choice of age model is also supported by the D_e distribution characteristics of the two samples, which are typified by broad, unimodal, symmetric D_e dispersion. Such properties are not consistent with the distinctive positively skewed D_e distributions reported elsewhere for partially bleached sediments (e.g., Arnold et al., 2009) and indicate that a measure of central tendency is likely to adequately represent the dispersion in these D_e datasets. Taken together, the CAM ages of these samples indicate an MIS 6 age for the Reid glaciation.

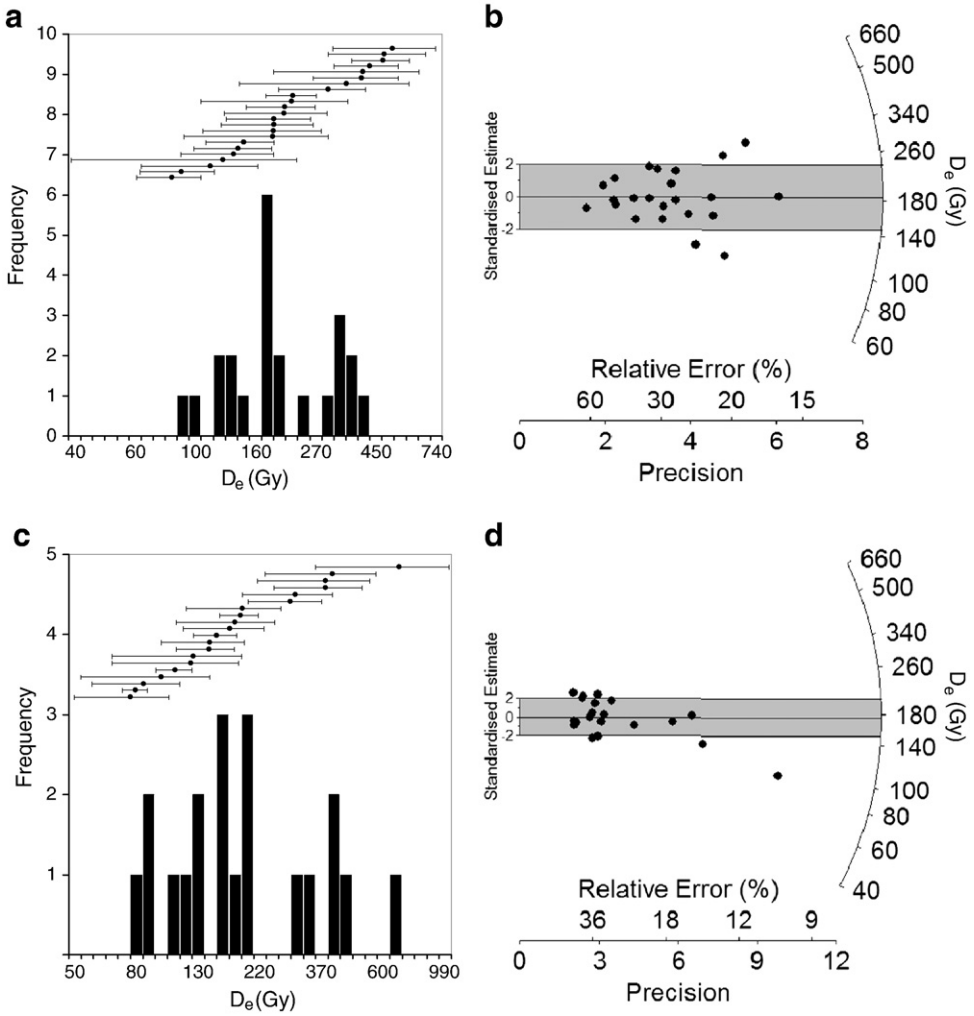

Figure 5. D_e frequency distributions with ranked D_e estimates plotted on a log scale and radial plots obtained from single grains of quartz for sample 57A (a–b), and sample 58A (c–d). The shaded bar in (b) and (d) is centred on the central age model (CAM) D_e estimate.

https://doi.org/10.1016/j.yqres.2011.11.009 Published online by Cambridge University Press

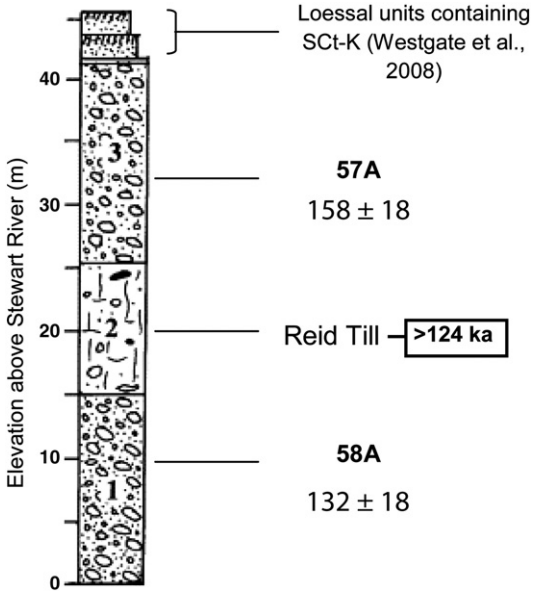

Figure 6. Final single-grain OSL ages obtained for glaciofluvial gravels bracketing Reid till at Ash Bend.

Moreover, these ages preclude a MIS 8 age for the Reid deposits at Ash Bend and, in addition to providing a robust minimum age constraint on the Reid glaciation, provide the first direct maximum age constraint on the Reid deposits in central Yukon.

It is worth noting that the OSL ages obtained using the dose rate values calculated from the as-measured water contents are significantly younger than independent ages obtained for the overlying SCt-K at Ash Bend and the Old Crow tephra, which overlies Selwyn lobe deposits elsewhere (Ward et al., 2008; Table S2). The CAM ages obtained using the as-measured water contents decrease by ~25% to 120 ± 13 ka for sample 57A and decrease by ~15% to 113 ± 15 ka for sample 58A (Table S2). Both these ages correspond to the MIS 5 interglacial and are inconsistent with the stratigraphic position of the Reid gravels below the ~124 ka Old Crow tephra elsewhere (Ward et al., 2008). The corresponding MAM-3 and MAM-4 ages for samples 57A and 58A range between ~63 ka and ~90 ka (Table S2). These are all younger than the ~124 ka Old Crow tephra age and, in the case of sample 58A, underestimate the ~80 ka SCt-K, which overlies the samples at the site. The inconsistency of these results confirms the inappropriateness of using the as-measured water contents for these samples and provides further support for our selection of the saturated water contents in the final age calculations. While understanding that minor uncertainty exists in our long-term water content estimate for these samples, we note that adopting an 80% degree of saturation instead of the full saturated water content does not change the final MIS 6 age estimates beyond their existing error ranges (Table S2). The OSL ages for the Reid deposits are therefore relatively insensitive to our selection of long-term water content (within a reasonable range of expected values for sand-rich permafrost sediments; e.g., Iwasaki et al., 2010), particularly as the assigned uncertainty terms already accounts for unexpected deviations of up to 15% in the long-term moisture content.

Discussion

Single-grain OSL dating has been successfully applied to glaciofluvial deposits from the Reid glaciation in northwest Canada (easternmost Beringia). The OSL properties of individual quartz grains were suitable for deriving burial ages, in spite of the generally low signal intensities of the grains measured. The MIS 6 ages obtained for the Reid glaciation at its reference locale in central Yukon agree with independent chronologies from the overlying Old Crow tephra (124 ± 10 ka) (Ward et al., 2008), as well as with cosmogenic ages from glacial deposits belonging to the Selwyn lobe expansion at a nearby site (Stroeven et al., 2010).

The OSL results obtained in this study are significant from both a methodological and palaeoenvironmental perspective. In particular, our findings add to the growing body of OSL dating research on glacial deposits and provide new insights into the potential for using single-grain techniques to reconstruct glacial histories in this region. The new minimum and maximum age constraints on the Reid till also have a broader significance for understanding the complex regional glacial history of eastern Beringia. We go on to discuss in further detail these two aspects of our findings in the following sections.

Implications for single-grain OSL dating of glacial deposits in eastern Beringian

Several OSL dating studies of glacigenic deposits undertaken at both the multi-grain and single-grain scale of analysis have reported similar problems of low quartz signal intensity (Rhodes, 2000; Duller, 2006; Klasen et al., 2006, 2007; Lukas et al., 2007; Namara et al., 2007; Preusser et al., 2007; Demuro et al., 2008). Indeed, a number of researchers have opted to use 'brighter' IRSL emissions of feldspar extracts to overcome the problems of quartz 'dimness' in glacigenic contexts (e.g., Tsukamoto et al., 2002; Spencer and Owen, 2004). Comparisons with independent age control have revealed that these types of depositional environments may be prone to partial bleaching (Spencer and Owen, 2004; Duller, 2006; Preusser et al., 2007; Houmark-Nielsen, 2008), although several known-age studies have also indicated that sufficient resetting of quartz OSL signals is possible for certain glacigenic deposits such as moraines, tills and glaciofluvial sediments (Tsukamoto et al., 2002; Thomas et al., 2006; Bøe et al., 2007; Namara et al., 2007).

For glaciofluvial deposits, the extent of bleaching at deposition will vary considerably depending on transportation distances, environmental conditions (e.g., water depth, turbidity, sediment load, sediment size) and sunlight exposure (e.g., daylight intensities, spectra, duration). As such, it is inappropriate to generalise about the bleaching conditions of any given glaciofluvial sample on the basis of its depositional context alone. Moreover, direct comparison of bleaching trends between the aforementioned studies and the Reid glaciofluvial sediments is not straightforward because, with the exception of Duller (2006) and Bøe et al. (2007), they have all used multi-grain aliquots (typically containing several thousand grains), which are apt to 'mask' the true signatures of insufficient bleaching in final D_e estimates.

Recent single-grain OSL dating studies of quartz from glacigenic sediments have been instrumental in revealing just how diverse bleaching conditions can be in this environmental setting. Duller (2006) was the first study to report single-grain OSL dating of glaciogenic gravels. The study included an assessment of single-grain OSL dating at two geographically separate sites (Chile and Scotland). With the aid of independent age control, Duller (2006) found that the single-grain D_e distributions of 8 glaciofluvial samples ranged from being generally well-bleached to very poorly bleached and that the lowest D_e populations, obtained using the finite mixture model (FMM) of Galbraith and Green (1990), produced ages in agreement with cosmogenic and radiocarbon ages. Elsewhere, Bøe et al. (2007) examined the single-grain D_e distributions of 3 glaciofluvial samples from central Norway as part of a larger multiple-grain aliquot OSL dating study. In contrast to the results of Duller (2006), the single-grain D_e datasets reported by Bøe et al. (2007) were all indicative of sufficient daylight exposure during transportation. The overdispersion values of these single-grain D_e distributions were very low (5–9%) and weighted mean ages obtained at the single-grain and multiple-grain scale of analysis were consistent, providing further support that these glaciofluvial samples had been fully bleached at deposition.

https://doi.org/10.1016/j.yqres.2011.11.009 Published online by Cambridge University Press

The single-grain OSL results obtained in the present study are somewhat distinct from those of Duller (2006) and Bøe et al. (2007), and confirm that a broad array of D_e distribution characteristics can be encountered in glaciofluvial contexts. Although the D_e values are spread over a rather large range and have high overdispersion values, they do not display a dominant leading-edge or statistically significant positive skewness. These characteristics imply that either (i) partial bleaching is not a dominant source of D_e scatter for these samples or that (ii) these samples were very poorly bleached at deposition and only a few grains had their residual OSL signals fully reset prior to burial. Importantly, the latter seems unlikely in this case because the final D_e estimates calculated using a measure of central tendency (the CAM) produce ages that are in agreement with the independent minimum age control of ~124 ka; this would not be expected if the weighted mean ages were derived from populations of grains containing residual doses. However, it should be pointed out that the D_e datasets of sample 57A and 58A are rather limited in number ($n \approx 20$) due to the low number of grains passing the SAR rejection criteria, and that further D_e measurements ideally would be needed to fully clarify the statistical attributes of these single-grain dose distributions.

In comparing the present study to previous single-grain studies of glaciofluvial deposits, it should also be remembered that the influence of partial bleaching is likely to be much more apparent in younger samples than older ones, mainly because the residual doses associated with unbleached grains can be much larger in relative terms compared to the mean burial dose of fully bleached grains. The samples studied by Duller (2006) and Bøe et al. (2007) yielded ages of ~2–17 ka and ~14–20 ka, respectively, and hence were considerably younger than those presented here. The antiquity of our samples is likely to account, at least partly, for their distinctive D_e distribution characteristics and the seemingly minimal (or non-existent) influence of partial bleaching. Significantly, however, our broadly dispersed D_e datasets demonstrate that older (late Pleistocene) samples are not immune from the influences of extrinsic and/or intrinsic sources of D_e scatter. We provide additional discussion of the possible sources of this D_e scatter in the Supplementary material. Our assessment suggests that the relatively high dispersion in these D_e datasets may be attributable to beta-dose heterogeneity in the sedimentary environment and/or intrinsic scatter arising from the experimental procedures and grain-to-grain variability in luminescence properties. However, it remains difficult to elucidate the specific source(s) of dose overdispersion affecting these samples without making further single-grain D_e measurements or without undertaking detailed comparative OSL studies with similar quartz samples from the region.

Implication for regional glacial reconstructions in eastern Beringia

The MIS 6 OSL ages for the Reid glaciation are consistent with chronologies obtained on several other glacial deposits across central Alaska and Yukon Territory. Specifically, at least two other glaciations have been assigned to MIS 6 in the region: the Delta glaciation in central Alaska (Begét and Keskinen, 2003) (Fig. 7), and possibly the Mirror Creek glaciation in southwestern Yukon Territory (Ward et al., 2008).

The Delta glaciation deposits, composed of outwash terraces extending downstream from the moraine, have been found overlain by the Old Crow tephra and in association with reworked Sheep Creek tephra deposits at the Moose Creek site along the Tanana River, central Alaska. Begét and Keskinen (2003) suggested a MIS 6 age for the Delta glaciation based on a maximum age estimate of ~190 ka on the SCt-F (Berger et al., 1996), and a minimum age constraint of ~124 ka from the overlying Old Crow tephra. Westgate et al. (2008) have recently revised the identification of the SCt-F tephra deposit at this site and have correlated it with a similar but distinct bed, the SCt-CC. Although the age of SCt-CC is not well constrained, the presence of the Old Crow tephra suggests a MIS 6 age for the prominent terrace below the Delta limit. Seemingly contradictory ages were, however, obtained by Matmon et al. (2010) using cosmogenic dating of Delta glaciation moraines from the Donnelly Dome area of the Delta River valley. Though these moraines lack large boulders that are most suitable for cosmogenic dating, the results of Matmon et al. (2010) suggested MIS 4 ages for the Delta drift deposits. However, the ^{10}Be exposure ages presented in that study were widely dispersed (~12–70 ka), and their chronological significance remains unclear in light of the potential for post-depositional exhumation of the moraine. On the basis of the current tephrochronology and stratigraphic evidence at Moose Creek, there is a strong argument for an extensive ice-sheet advance during MIS 6, and a potentially similarly extensive glaciation during MIS 4 if the ages of Matmon et al. (2010) are considered reliable estimates of the full exposure time of the moraine deposits. Given the tephrochronological constraint, however, it appears likely that the advance of the Delta lobe occurred during MIS 6, which would make the Delta glaciation contemporaneous with the Reid glaciation ages derived in the present study for central Yukon.

The Mirror Creek glaciation (the St. Elias lobe of the Cordilleran Ice Sheet in southwestern Yukon Territory) has been tentatively assigned to MIS 6, but no firm chronology exists for these glacial deposits. Rampton (1971) first described the Mirror Creek glaciation deposits in the Snag–Klutlan area (Fig. 1). There, glacial deposits have been assigned to MIS 6 on the basis of their stratigraphic relations with overlying Old Crow tephra deposits (Westgate et al., 1985; Ward et al., 2008). However, the Mirror Creek glacial deposits currently lack a tight maximum age constraint, so it is not possible to rule out an earlier (i.e., MIS 8) age for the penultimate advance of the Cordilleran Ice Sheet in this area. While the results of the present study indicate that the Reid deposits at Ash Bend might be temporally correlated with those in the Snag-Klutlan area, this cannot be stated definitively without improved chronological constraints on the Mirror Creek deposits.

Elsewhere across eastern Beringia, several other glacial deposits related to the penultimate advance have been assigned to MIS 4 rather than MIS 6 (Briner et al., 2005). In particular, the St. Elias lobes of the Cordilleran Ice Sheet are thought to have reached their penultimate limit during MIS 4 in the Aishihik Lake area, southwest Yukon Territory (Ward et al., 2007) (Fig. 7). Farther afield, there is strong evidence to suggest that several other regions across the Beringian sub-continent experienced more extensive glacial advances during MIS 4 or late MIS 5 compared to MIS 2 (Kaufman et al., 1996, 2001; Briner et al., 2005; Elias and Brigham-Grette, 2007) (Fig. 7). When considered in combination with the ages presented here, these pre-last glacial maximum (LGM) glacial chronologies suggest that sediments associated with the penultimate glacial advances were not deposited synchronously across eastern Beringia (or across the broader Beringian sub-continent): glaciers that were situated close to coastal regions (e.g., western Alaska and southern Yukon) may have expanded further than glaciers in more continental regions (e.g., Alaskan Range and central Yukon Territory) during late MIS 5 and MIS 4. In contrast, continental areas such as central Yukon may have experienced more prominent glacial advances during MIS 6; the lack of identifiable deposits between the MIS 2 and 6 limits in some of these areas, such as the Selwyn lobe considered here, would suggest that the MIS 4 advance was in fact less extensive than the LGM limit.

Summary

1. The results obtained in this study reveal that single-grain OSL techniques are well-suited for dating deposits of glacial origin, and that these approaches offer significant potential for reconstructing glacial histories in eastern Beringia. The low yield of quartz grains displaying suitable properties for OSL dating

https://doi.org/10.1016/j.yqres.2011.11.009 Published online by Cambridge University Press

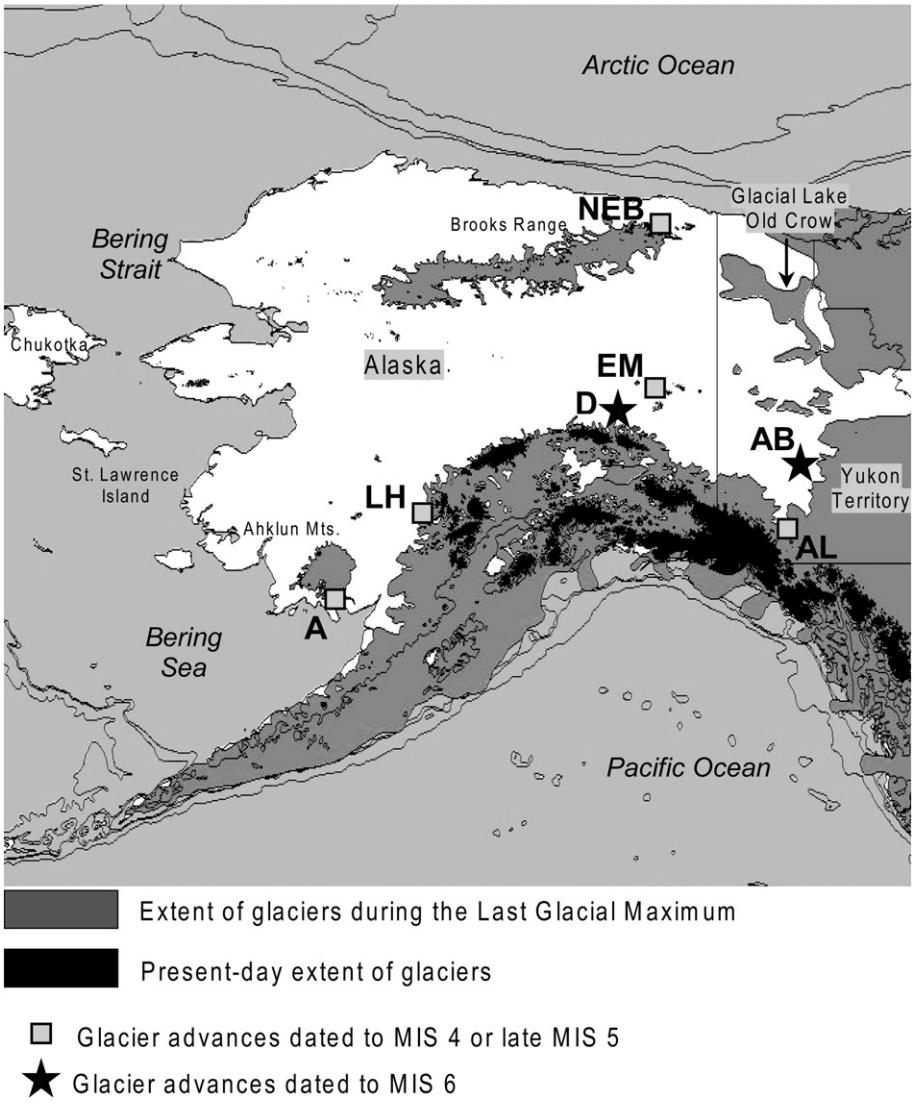

Figure 7. Sites in central and eastern Beringia where the maximum glacier advances prior to MIS 2 have been dated to MIS 4 or late MIS 5 (squares) and to MIS 6 (stars). Indicated are: Ahklun Mountains (A), Lime Hills region, western Alaskan Range (LH), Delta Glaciation site (D), Eagle Moraine (EM), northeastern Brooks Range (NEB), Aishihik Lake area (AL), Ash Bend site (AB). (Data from: Kaufman et al., 2001; Begét and Keskinen, 2003; Briner et al., 2005; Ward et al., 2007).

(~1% of the total measured grains) underscores the importance of applying single-grain techniques in this study. This approach is the only means of ensuring that the large numbers of grains displaying aberrant or unreliable luminescence properties do not contribute to the final age estimates. We encourage more widespread application of single-grain dating in future OSL studies of similar late Quaternary glacigenic sediments.

2. We have obtained two OSL ages of 132 ± 18 ka and 158 ± 18 ka for the gravel units underlying and overlying the Reid till, respectively. These ages represent the first combined minimum and maximum chronological constraint on the Reid glaciation of the central Yukon Territory.
3. The new OSL ages of the Reid drift samples are consistent with existing minimum ages for associated, overlying tephra deposits, namely the Old Crow tephra (~124 ka), found above the Reid gravels along the Pelly River, and the SCt-K tephra (~80 ka), found in the overlying loess section at Ash Bend.
4. The weighted mean OSL age for the Reid till in central Yukon is 150 ± 10 ka and places the Reid glaciation within MIS 6. The new single-grain OSL chronology precludes a MIS 8 age for the Reid glaciation in central Yukon Territory. This finding facilitates improved interpretations of regional glacial histories in eastern Beringia. In particular, the OSL chronology is consistent with reconstructions of glacial advances in central Alaska for the Delta glaciation, which has been assigned to MIS 6, and indicates that the Reid glacial deposits are likely correlative with the Mirror Creek glaciation deposits in southern Yukon Territory. Our MIS 6 ages also confirm that glacial deposits corresponding to the penultimate maximum glacial advance in eastern Beringia represent a diachronous record in need of site-specific chronological constraints, since several other sites in the region contain penultimate glacial deposits dating to MIS 4.

Acknowledgments

We thank the Australian Research Council for a Discovery Project grant (DP0558446) to R.G.R., the University of Wollongong for a University Postgraduate Award to M.D., and the Natural Science and Engineering Research Council for a grant to D.F. This research was partly supported by a Marie Curie International Reintegration Grant (PIRG08-GA-2010-276810) awarded to M.D. within the 7th European Community Framework Programme.

https://doi.org/10.1016/j.yqres.2011.11.009 Published online by Cambridge University Press

Appendix A. Supplementary Data

Supplementary data to this article can be found online at doi:10.1016/j.yqres.2011.11.009.

References

Adamiec, G., Aitken, M., 1998. Dose-rate conversion factors: update. Ancient TL 16, 37–50.

Aitken, M.J., 1985. Thermoluminescence Dating. Academic Press, London. 359 pp.

Aitken, M.J., 1998. An Introduction to optical dating: the dating of quaternary sediments by the use of photon-stimulated luminescence. Oxford University Press, Oxford. 267 pp.

Arnold, L.J., Roberts, R.G., 2009. Stochastic modelling of multi-grain equivalent dose (D_e) distributions: implications for OSL dating of sediment mixtures. Quaternary Geochronology 4, 204–230.

Arnold, L.J., Roberts, R.G., Galbraith, R.F., DeLong, S.B., 2009. A revised burial dose estimation for optical dating of young and modern-age sediments. Quaternary Geochronology 4, 306–325.

Bailey, R.M., Arnold, L.J., 2006. Statistical modelling of single grain quartz D_e distributions and an assessment of procedures for estimating burial dose. Quaternary Science Reviews 25, 2475–2502.

Begét, J.E., Keskinen, M.J., 2003. Trace-element geochemistry of individual glass shards of the Old Crow tephra and the age of the Delta glaciation, central Alaska. Quaternary Research 60, 63–69.

Berger, G.W., Péwé, T.L., Westgate, A.G., Preece, S.J., 1996. Age of Sheep Creek tephra (Pleistocene) in central Alaska from thermoluminescence dating of bracketing loess. Quaternary Research 45, 263–270.

Bøe, A.-G., Murray, A., Dhal, S.O., 2007. Resetting of sediments mobilised by the LGM ice-sheet in southern Norway. Quaternary Geochronology 2, 222–228.

Bostock, H.S., 1966. Notes on glaciation in central Yukon Territory. Geological Survey of Canada, Paper 65–36. .

Bøtter-Jensen, L., Andersen, C.E., Duller, G.A.T., Murray, A.S., 2003. Developments in radiation, stimulation and observation facilities in luminescence measurements. Radiation Measurements 37, 535–541.

Bowler, J.M., Johnston, J., Olley, J.M., Prescott, J.R., Roberts, R.G., Shawcross, W., Spooner, N.A., 2003. New ages for human occupation and climatic change at Lake Mungo, Australia. Nature 421, 837–840.

Briner, J.P., Kaufman, D.S., Manley, W.F., Finkel, R.C., Caffee, M.W., 2005. Cosmogenic exposure dating of late Pleistocene moraine stabilization in Alaska. Geological Society of America Bulletin 117, 1108–1120.

Demuro, M., Roberts, R.G., Froese, D.G., Arnold, L.J., Brock, F., Bronk Ramsey, C., 2008. Optically stimulated luminescence dating of single and multiple grains of quartz from perennially frozen loess in western Yukon Territory, Canada: comparison with radiocarbon chronologies for the late Pleistocene Dawson tephra. Quaternary Geochronology 3, 346–364.

Duk-Rodkin, A., 1999. Glacial limits map of Yukon Territory. Geological Survey of Canada Open File 3288 and Yukon Geological Survey Open File 1999–2, 1:1,000,000 scale. .

Duk-Rodkin, A., Barendregt, R.W., 2011. Chapter 49 — startigraphical record of glacials/interglacials in Northwest Canada. Developments in Quaternary Sciences 15, 661–698.

Duk-Rodkin, A., Barendregt, R.W., White, J.M., 2010. An extensive late Cenozoic terrestrial record of multiple glaciations preserved in the Tintina Trench of west-central Yukon: stratigraphy, paleomagnetism, paleosols, and pollen. Canadian Journal of Earth Sciences 47, 1003–1028.

Duller, G.A.T., 2003. Distinguishing quartz and feldspar in single grain luminescence measurements. Radiation Measurements 37, 161–165.

Duller, G.A.T., 2006. Single grain optical dating of glacigenic deposits. Quaternary Geochronology 1, 296–304.

Duller, G.A.T., 2007. Assessing the error on equivalent dose estimates derived from single aliquot regenerative dose measurements. Ancient TL 25, 15–24.

Duller, G.A.T., 2008. Single-grain optical dating of Quaternary sediments: why aliquot size matters in luminescence dating. Boreas 37, 589–612.

Elias, S.A., Brigham-Grette, J., 2007. Late Pleistocene events in Beringia. In: Elias, S.A. (Ed.), Encyclopedia of Quaternary Science. Elsevier, pp. 1057–1066.

Froese, D.G., Barendregt, R.W., Enkin, R.J., Baker, J., 2000. Paleomagnetism of Late Cenozoic terraces of the lower Klondike Plateau valley: evidence for multiple Late Pliocene–Early Pleistocene glaciations. Canadian Journal of Earth Sciences 37, 863–877.

Galbraith, R.F., Green, P.F., 1990. Estimating the component ages in a finite mixture. Nuclear Tracks and Radiation Measurements 17, 197–206.

Galbraith, R.F., Roberts, R.G., Laslett, G.M., Yoshida, H., Olley, J.M., 1999. Optical dating of single and multiple grains of quartz from Jinmium rock shelter, northern Australia: part I, experimental design and statistical models. Archaeometry 41, 339–364.

Galbraith, R.F., Roberts, R.G., Yoshida, H., 2005. Error variation in OSL palaeodose estimates from single aliquots of quartz: a factorial experiment. Radiation Measurements 39, 289–307.

Goehring, B.M., Brook, E.J., Linge, H., Raisbeck, G.M., Yiou, F., 2008. Beryllium-10 exposure ages of erratic boulders in southern Norway and implications for the history of the Fennoscandian Ice Sheet. Quaternary Science Reviews 27, 320–336.

Hansen, L., Funder, S., Murray, A.S., Mejdahl, V., 1999. Luminescence dating of the last Weichselian Glacier advance in East Greenland. Quaternary Geochronology 18, 179–190.

Houmark-Nielsen, M., 2008. Testing OSL failures against a regional Weichselian glaciation chronology from southern Scandinavia. Boreas 37, 660–677.

Hughes, O.L., Campebell, R.B., Muller, J.E., Wheeler, J.O., 1969. Glacial limits and flow patterns, Yukon Territory, South of 65 degrees North latitude. Geological Survey of Canada, Paper 68–34. .

Hughes, O.L., Harington, C.R., Schweger, C., Matthews Jr., J.V., 1987. Stop 15: Ash Bend Section. In: Morrison, S.R., Smith, C.A.S. (Eds.), Guidebook for Quaternary research in Yukon. : XII International Union for Quaternary Research (INQUA) Congress, Ottawa, Ont. National Research Council of Canada, Ottawa, Ont., pp. 50–53.

Huscroft, C.A., Ward, B.C., Barendregt, R.W., Jackson Jr., L.E., Opdyke, N.D., 2004. Pleistocene volcanic damming of Yukon River and the maximum age of the Reid Glaciation, west-central Yukon. Canadian Journal of Earth Sciences 41, 151–164.

Iwasaki, H., Saito, H., Kuwao, K., Maximov, T.C., Hasegawa, S., 2010. Forest decline caused by high water conditions in a permafrost region. Hydrology and Earth System Sciences 14, 301–307.

Kaufman, D.S., Manley, W.F., 2004. Pleistocene maximum and Late Wisconsin glacier extents across Alaska, U.S.A. In: Ehlers, J., Gibbard, P.L. (Eds.), Quaternary Glaciations — Extent and Chronology, Part II: North America. : Developments in Quaternary Science, 2b. Elsevier, Amsterdam, Netherlands, pp. 9–27.

Kaufman, D.S., Forman, S.L., Lea, P.D., Wobus, C.W., 1996. Age of pre-late-Wisconsin glacial-estuarine sedimentation, Bristol Bay, Alaska. Quaternary Research 45, 59–72.

Kaufman, D.S., Manley, W.F., Forman, S., Layer, P., 2001. Pre-late Wisconsin glacial history, coastal Ahklun Mountains, southwestern Alaska — new amino acid, thermoluminescence, and $^{40}Ar/^{39}Ar$ results. Quaternary Science Reviews 20, 337–352.

Klasen, N., Fiebig, M., Preusser, F., Radtke, U., 2006. Luminescence properties of glaciofluvial sediments from the Bavarian Alpine Foreland. Radiation Measurements 41, 866–870.

Klasen, N., Fiebig, M., Preusser, F., Reitner, J.M., Radtke, U., 2007. Luminescence dating of proglacial sediments from the Eastern Alps. Quaternary International 164–165, 21–32.

Lacelle, D., Lauriol, B., Clark, I.D., Cardyn, R., Zdanowicz, C., 2007. Nature and origin of Pleistocene-age massive ground-ice body exposed in the Chapman Lake moraine complex, central Yukon Territory, Canada. Quaternary Research 68, 249–260.

Lian, O.B., Hu, J., Huntley, D.J., Hicock, S.R., 1995. Optical dating studies of Quaternary organic-rich sediments from southwestern British Columbia and northwestern Washington State. Canadian Journal of Earth Sciences 32, 1194–1207.

Lukas, S., Spencer, J.Q.C., Robinson, R.A.J., Benn, D.I., 2007. Problems associated with luminescence dating of Late Quaternary glacial sediments in NW Scottish Highlands. Quaternary Geochronology 2, 243–248.

Matmon, A., Briner, J.P., Carver, G., Bierman, P., Finkel, R.C., 2010. Moraine chronosequence of the Donnelly Dome region, Alaska. Quaternary Research 74, 63–72.

Mejdahl, V., 1979. Thermoluminescence dating: beta-dose attenuation in quartz grains. Archaeometry 21, 61–72.

Murray, A.S., Wintle, A., 2000. Luminescence dating of quartz using an improved single-aliquot regenerative-dose protocol. Radiation Measurements 32, 57–73.

Murray, A.S., Wintle, A.G., 2003. The single aliquot regenerative dose protocol: potential for improvements and reliability. Radiation Measurements 37, 377–381.

Namara, C., Kondo, R., Tsukamoto, S., Kajiura, T., Ormukov, C., Abdrakhmatov, K., 2007. OSL dating of glacial deposits during the Last Glacial in the Terskey-Alatoo Range, Kyrgyz Republic. Quaternary Geochronology 2, 249–254.

Olley, J.M., Caircheon, G.G., Roberts, R.G., 1999. The origin of dose distributions in fluvial sediments, and the prospect of dating single grains from fluvial deposits using optically stimulated luminescence. Radiation Measurements 30, 207–217.

Olley, J.M., De Deckker, P., Roberts, R.G., Fifield, L.K., Yoshida, H., Hancock, G., 2004. Optical dating of deep-sea sediments using single grains of quartz: a comparison with radiocarbon. Sedimentary Geology 169, 175–189.

Péwé, T.L., 1975. The Quaternary geology of Alaska. U.S. geological Survey Professional Paper, 835.

Pigati, J.S., Quade, J., Wilson, J., Jull, A.J.T., Lifton, N.A., 2007. Development of low-background vacuum extraction and graphitization systems for 14C dating of old (40–60 ka) samples. Quaternary International 166, 4–14.

Preece, S.J., Pearce, N.J.G., Westgate, J.A., Froese, D.G., Jensen, B.J.L., Perkins, W.T., 2011. Old Crow tephra across eastern Beringia: a single cataclysmic eruption at the close of Marine Isotope Stage 6. Quaternary Science Reviews 30, 2069–2090.

Prescott, J.R., Hutton, J.T., 1994. Cosmic ray contributions to dose rates for luminescence and ESR dating: large depths and long-term time variations. Radiation Measurements 23, 497–500.

Preusser, F., Blei, A., Graf, H., Schlüchter, C., 2007. Luminescence dating of Würmian (Weichselian) proglacial sediments from Switzerland: methodological aspects and stratigraphical conclusions. Boreas 36, 130–142.

Rampton, V.N., 1971. Late Pleistocene glaciations in the Snag–Klutlan area, Yukon Territory. Arctic 24, 277–300.

Reyes, A.V., Jensen, B.J.L., Zazula, G.D., Ager, T.A., Kuzmina, S., La Farge, C., Froese, D.G., 2010. A late–Middle Pleistocene (marine isotope stage 6) vegetated surface buried by Old Crow tephra at the Palisades, interior Alaska. Quaternary Science Reviews 29, 801–811.

Rhodes, E.J., 2000. Observations of thermal transfer OSL signals in glacigenic quartz. Radiation Measurements 32, 595–602.

Schweger, C.E., 2003. Paleoecology of two marine oxygen isotope stage 7 sites correlated by Sheep Creek tephra, northwestern North America. Quaternary Research 60, 44–49.

Smith, C.A.S., Tarnocai, C., Hughes, O.L., 1986. Pedological investigations of Pleistocene glacial drift surfaces in the central Yukon. Géographie Physique et Quaternaire 40, 29–37.

Spencer, J.Q., Owen, L.A., 2004. Optically stimulated luminescence dating of Late Quaternary glaciogenic sediments in the upper Hunza Valley: validating the timing of glaciation and assessing dating methods. Quaternary Science Reviews 23, 175–191.

Stokes, S., Ingram, S., Aitken, M.J., Sirocko, F., Anderson, R., Leuschner, D., 2003. Alternative chronologies for Late Quaternary (Last Interglacial–Holocene) deep sea sediments via optical dating of silt-sized quartz. Quaternary Science Reviews 22, 925–941.

Stroeven, A.P., Fabel, D., Codilean, A.T., Kleman, J., Clague, J.J., Miguens-Rodriguez, M., Xu, S., 2010. Investigating the glacial history of the northern sector of the Cordilleran Ice Sheet with cosmogenic 10Be concentrations in quartz. Quaternary Science Reviews 29, 3630–3643.

Thomas, P.J., Murray, A.S., Kjær, K.H., Funder, S., Larsen, E., 2006. Optically stimulated luminescence (OSL) dating of glacial sediments from Arctic Russia — depositional bleaching and methodological aspects. Boreas 35, 587–599.

Tsukamoto, S., Asahi, K., Watanabe, T., Rink, W.J., 2002. Timing of past glaciations in Kanchenjunga Himal, Nepal by optically stimulated luminescence dating of tills. Quaternary International 97–98, 57–67.

Ward, B.C., Bond, J.D., Gosse, J.C., 2007. Evidence for a 55–50 ka (early Wisconsin) glaciation of the Cordilleran Ice Sheet, Yukon Territory, Canada. Quaternary Research 68, 141–150.

Ward, B.C., Bond, J.D., Froese, D., Jensen, B., 2008. Old Crow tephra (140 ± 10 ka) constrains penultimate Reid glaciation in central Yukon Territory. Quaternary Science Reviews 27, 1909–1915.

Westgate, J.A., Walter, R.C., Pearce, G.W., Gorton, M.P., 1985. Distribution, stratigraphy, petrochemistry, and palaeomagnetism of the late Pleistocene Old Crow tephra in Alaska and the Yukon. Canadian Journal of Earth Sciences 22, 893–906.

Westgate, J.A., Preece, S.J., Froese, D.G., Walter, R.C., Sandhu, A.S., Schweger, C.E., 2001. Dating early and middle (Reid) Pleistocene glaciations in central Yukon by tephrochronology. Quaternary Research 56, 335–348.

Westgate, J.A., Preece, S.J., Froese, D.G., Pearce, N.J.G., Roberts, R.G., Demuro, M., Hart, W.K., Perkins, W., 2008. Changing ideas on the identity and stratigraphic significance of the Sheep Creek tephra beds in Alaska and the Yukon Territory, northwestern North America. Quaternary International 178, 183–209.

Wintle, A.G., Murray, A.S., 2006. A review of quartz optically stimulated luminescence characteristics and their relevance in single-aliquot regeneration dating protocols. Radiation Measurements 41, 369–391.

https://doi.org/10.1016/j.yqres.2011.11.009 Published online by Cambridge University Press